

# Iterative Optimization in Medical Imaging

Charles Byrne

(Charles\_Byrne@uml.edu)

<http://faculty.uml.edu/cbyrne/cbyrne.html>

Department of Mathematical Sciences

University of Massachusetts Lowell

Lowell, MA 01854, USA

March 12, 2008

# Acknowledgments

This work was supported, in part, by the National Institutes of Health (NIH), under grant CA23452. The contents of this presentation are solely the responsibility of the author and do not necessarily reflect the official views of NIH.

## Talk Available on Web Site

This slide presentation and accompanying article are available on my web site, <http://faculty.uml.edu/cbyrne/cbyrne.html> ; click on “Talks”.

# Overview

- 1. transmission tomography and non-iterative filtered backprojection;
- 2. discretization and iteration- ART and MART;
- 3. emission tomography and iterative likelihood maximization;
- 4. the EMMML algorithm for emission tomography;
- 5. acceleration through block-iterative methods;
- 6. iterative entropy maximization;
- 7. the split feasibility problem and the CQ algorithm;
- 8. intensity-modulated radiation therapy (IMRT).

# Transmission Tomography

In transmission tomography, radiation, usually x-ray, is transmitted along many lines through the object of interest and the initial and final intensities are measured. The intensity drop associated with a given line indicates the amount of attenuation the ray encountered as it passed along the line. It is this distribution of attenuating matter within the patient, described by a function of two or three spatial variables, that is the object of interest. Unexpected absence of attenuation can indicate a break in a bone, for example. The data are usually modeled as line integrals of that function. The Radon transform is the function that associates with each line its line integral.

## Drop in X-ray Intensity Along Line $L$

The intensity of the x-ray beam upon entry is  $I_{in}$  and  $I_{out}$  is its lower intensity after passing through the body, along line  $L$ . Then we have

$$I_{out} = I_{in} e^{-\int_L f}, \quad (1)$$

where  $f = f(x, y) \geq 0$  is the *attenuation function* describing the two-dimensional distribution of matter within the slice of the body being scanned and  $\int_L f$  is the integral of the function  $f$  over the line  $L$  along which the x-ray beam has passed.

# The Exponential-Decay Model

The line  $L$  is parameterized by the variable  $s$  and the intensity function is  $I(s)$ . For small  $\Delta s > 0$ , the drop in intensity from the start to the end of the interval  $[s, s + \Delta s]$  is approximately proportional to the intensity  $I(s)$ , to the attenuation  $f(s)$  and to  $\Delta s$ , the length of the interval; that is,

$$I(s) - I(s + \Delta s) \approx f(s)I(s)\Delta s. \quad (2)$$

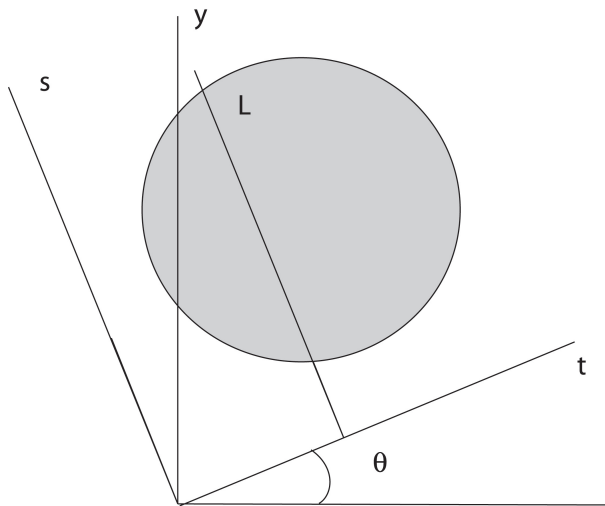
Dividing by  $\Delta s$  and letting  $\Delta s$  approach zero, we get

$$I'(s) = -f(s)I(s), \quad (3)$$

and so

$$I(s) = I(0) \exp\left(-\int_{u=0}^{u=s} f(u) du\right).$$

# Radon Transform



# The Radon Transform

For each fixed value of  $t$ , we compute the integral

$$\int_L f(x, y) ds = \int f(t \cos \theta - s \sin \theta, t \sin \theta + s \cos \theta) ds \quad (5)$$

along the single line  $L$  corresponding to the fixed values of  $\theta$  and  $t$ . We repeat this process for every value of  $t$  and then change the angle  $\theta$  and repeat again. We denote by  $r_f(\theta, t)$  the integral

$$r_f(\theta, t) = \int_L f(x, y) ds. \quad (6)$$

The function  $r_f(\theta, t)$  is called the *Radon transform* of  $f$ .

# The Central Slice Theorem

For fixed  $\theta$  the function  $r_f(\theta, t)$  is a function of the single real variable  $t$ ; let  $R_f(\theta, \omega)$  be its Fourier transform. Then

$$R_f(\theta, \omega) = \int r_f(\theta, t) e^{i\omega t} dt \quad (7)$$

$$= \int \int f(t \cos \theta - s \sin \theta, t \sin \theta + s \cos \theta) e^{i\omega t} ds dt \quad (8)$$

$$= \int \int f(x, y) e^{i\omega(x \cos \theta + y \sin \theta)} dx dy = F(\omega \cos \theta, \omega \sin \theta), \quad (9)$$

where  $F(\omega \cos \theta, \omega \sin \theta)$  is the two-dimensional Fourier transform of the function  $f(x, y)$ , evaluated at the point  $(\omega \cos \theta, \omega \sin \theta)$ ; this relationship is called the *Central Slice Theorem*.

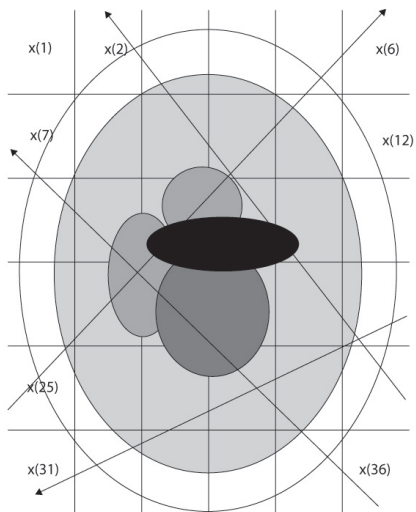
# Filtered Backprojection

For fixed  $\theta$ , as we change the value of  $\omega$ , we obtain the values of the function  $F$  along the points of the line making the angle  $\theta$  with the horizontal axis. As  $\theta$  varies in  $[0, \pi)$ , we get all the values of the function  $F$ . Once we have  $F$ , we can obtain  $f$  using the formula for the two-dimensional inverse Fourier transform:

$$f(x, y) = \frac{1}{4\pi^2} \int \int F(u, v) e^{-i(xu+yv)} du dv. \quad (10)$$

The *filtered backprojection* methods commonly used in the clinic are derived from different ways of calculating the double integral in Equation (10).

# The Discrete Model



# The Discrete Model

The estimated attenuation function will ultimately be reduced to a finite array of numbers prior to display. This discretization can be performed at the end, or can be made part of the problem model from the start. In the latter case, the attenuation function is assumed to be constant over small pixels or voxels; these constants are the object of interest now. The problem has been reduced to solving a large system of linear equations, possibly subject to non-negativity or other constraints.

# A Statistical Approach

If the physical nature of the radiation is described using a statistical model, then the pixel values can be viewed as parameters to be estimated. The well-known maximum likelihood parameter estimation method can then be employed to obtain these pixel values. This involves a large-scale optimization of the likelihood function.

# Discretization

For  $j = 1, \dots, J$ , let  $x_j$  be the unknown constant value of the attenuation function within the  $j$ th pixel or voxel.

For  $i = 1, \dots, I$ , let  $L_i$  be the set of pixel indices  $j$  for which the  $j$ th pixel intersects the  $i$ -th line segment, let  $|L_i|$  be the cardinality of the set  $L_i$ .

Let  $b_i > 0$  be the measured approximation of the line integral of  $f$  along  $L_i$ .

Let  $A_{ij} = 1$  for  $j$  in  $L_i$ , and  $A_{ij} = 0$  otherwise.

The line integral is replaced by  $(Ax)_i = \sum_{j \in L_i} A_{ij} x_j$ .

The problem is then to solve  $Ax = b$ .

# Algebraic Reconstruction Technique (ART)

With  $i = k(\bmod l) + 1$ , the iterative step of the ART algorithm is

$$x_j^{k+1} = x_j^k + \frac{1}{|L_i|} (b_i - (Ax^k)_i), \quad (11)$$

for  $j$  in  $L_i$ , and

$$x_j^{k+1} = x_j^k, \quad (12)$$

if  $j$  is not in  $L_i$ . In each step of ART, we take the error,  $b_i - (Ax^k)_i$ , associated with the current  $x^k$  and the  $i$ -th equation, and distribute it equally over each of the pixels that intersects  $L_i$ . For the ART we do not require that the  $A_{ij}$ ,  $b_i$  or the  $x_j$  be non-negative.

## Solving $Ax = b$ with the ART

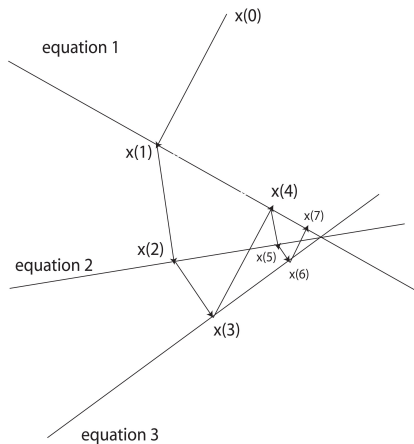
The ART can be used to solve any system of linear equations  $Ax = b$ . The iterative step of ART is

$$x_j^{k+1} = x_j^k + \frac{1}{\|a^i\|^2} (b_i - (Ax^k)_i) a^i, \quad (13)$$

where  $a^i$  denotes the  $i$ th column of  $A^\dagger$ .

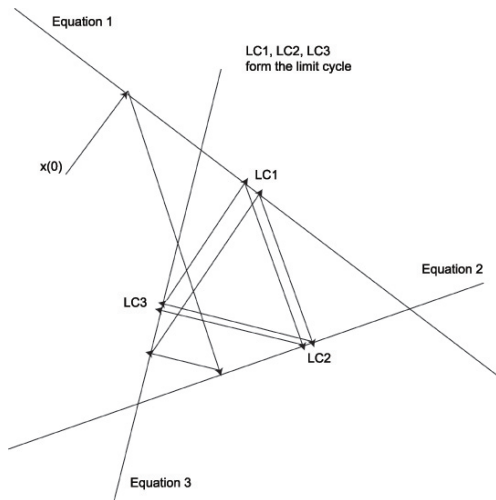
# ART: Consistent Case

In the consistent case, the ART converges to the solution closest to the starting vector.



# ART: The Inconsistent Case

In the inconsistent case, ART exhibits subsequential convergence to a limit cycle of distinct vectors.



# The Multiplicative ART (MART)

Suppose, now, that we have  $A_{ij} \geq 0$ ,  $b_i > 0$  and we know that the desired image we wish to reconstruct must be nonnegative. We can begin with  $x^0 > 0$ , but as we compute the ART steps, we may lose nonnegativity. One way to avoid this loss is to correct the current  $x^k$  multiplicatively, rather than additively, as in ART. This leads to the *multiplicative* ART (MART).

The MART, in this case, has the iterative step

$$x_j^{k+1} = x_j^k \left( \frac{b_i}{(Ax^k)_i} \right), \quad (14)$$

for those  $j$  in  $L_i$ , and

$$x_j^{k+1} = x_j^k, \quad (15)$$

otherwise. Therefore, we can write the iterative step as

$$x_j^{k+1} = x_j^k \left( \frac{b_i}{(Ax^k)_i} \right)^{A_{ij}}.$$

# The General MART

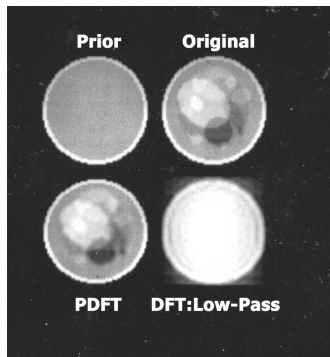
The MART can be used to solve systems of the form  $y = Px$ , where  $y$  has positive entries,  $P$  has non-negative entries, and we seek a non-negative solution. The iterative step of MART is

$$x_j^{k+1} = x_j^k \left( \frac{y_i}{(Px^k)_i} \right)^{P_{i,j}/m_i}, \quad (17)$$

where  $m_i = \max\{P_{i,j} \mid j = 1, \dots, J\}$ . If  $y = Px$  has non-negative solutions, then MART converges to such a solution; if not, MART exhibits subsequential convergence to a limit cycle, similar to ART.

# Using Prior Knowledge

If we take  $J$ , the number of pixels, to be larger than  $I$ , the number of measurements, then we have an under-determined problem, with multiple solutions. In such cases, prior knowledge can be used effectively to produce a reasonable reconstruction.



# Emission Tomography

In emission tomography, a carefully designed chemical tagged with a radioisotope is introduced into the body of the patient. The chemical is selected to accumulate in a specific organ or region of the body, such as the brain, or the heart wall. On the basis of emissions from the radioisotope that are detected outside the body, the distribution of the chemical within the body is estimated. Unexpected absence of the radionuclide from a given region, or a higher than expected concentration, can indicate a medical problem.

# PET and SPECT

There are two basic types of emission tomography:

- single photon emission computed tomography (SPECT);
- positron emission tomography (PET).

In SPECT the radioisotope emits a single photon, while in PET a positron is emitted, which shortly meets an electron and the resulting annihilation produces two gamma-ray photons traveling in essentially opposite directions.

# Randomness

In both SPECT and PET the data can be approximated as integrals along lines through the body and FBP used in reconstruction. However, more sophisticated models that more accurately describe the physics of the situation are preferred.

The photons that travel through the body toward the external detectors are sometimes absorbed by the body itself and not detected. The probability of being detected depends on the attenuation presented by the body. This attenuation, while not the object of interest now, is an important part of the physical model and needs to be included in the reconstruction method.

The randomness inherent in emission can also be included, leading once again to probabilistic models and a maximum likelihood approach to reconstruction.

# The Poisson Model in SPECT

The discrete model for emission tomography is the following:

- for  $j = 1, \dots, J$ ,  $x_j \geq 0$  is the unknown expected number of photons emitted from the  $j$ th pixel during the scan;
- for  $i = 1, \dots, I$ ,  $y_i > 0$  is the number of photons detected at the  $i$ th detector;
- $P_{ij} \geq 0$  is the probability that a photon emitted at  $j$  will be detected at  $i$ , which we shall assume is known;
- $s_j = \sum_{i=1}^I P_{ij}$  is the sensitivity to  $j$ , that is, probability that a photon emitted at  $j$  will be detected;
- the  $y_i$  are realizations of independent Poisson random variables with expected values  $(Px)_i = \sum_{j=1}^J P_{ij}x_j$ .

# Likelihood Maximization in SPECT

We view the unknown values  $x_j \geq 0$  as parameters to be estimated. To within a constant, the log of the likelihood function is then

$$LL(x) = \sum_{i=1}^I y_i \log(Px)_i - (Px)_i. \quad (18)$$

The EMLL algorithm for maximizing  $LL(x)$  over  $x \geq 0$  has the iterative step

$$x_j^{k+1} = x_j^k s_j^{-1} \sum_{i=1}^I P_{ij} \left( \frac{y_i}{(Px^k)_i} \right). \quad (19)$$

# Problems with the EMLL Algorithm

Although the EM algorithm allows for more accurate description of the physical situation, there are several disadvantages that must be removed before the EM algorithm can be a useful clinical tool:

- Calculating  $(Px^k)_i = \sum_{j=1}^J P_{ij}x_j^k$ , for each  $i$ , at each step of the iteration is expensive, since  $I$  and  $J$  can be in the tens of thousands;
- The sequence  $\{x^k\}$  usually converges quite slowly to the maximizer of  $LL(x)$ ;
- The maximum-likelihood (ML) solution will be a non-negative solution of  $y = Px$ , in the consistent case, that is, if such solutions exist, so may overfit noisy data;
- The ML solution may not be a good choice, in the inconsistent case, either.

# Controlling Noise

It can be shown that, when the system  $y = Px$  has no non-negative solutions, the maximum-likelihood solution will have at most  $l - 1$  non-zero pixel values, so, if  $J$  is greater than  $l$ , the ML solution may be useless. To control noise and obtain a useful image, one usually uses *regularization*, which means maximizing the sum of the likelihood function and another penalty function that is larger when the image is smooth.

# Acceleration

In the early 1990's it was noticed that if, when performing one step of the EM iteration, one summed only over some of the detector indices, instead of over all of them, one could usually obtain a useful reconstruction more quickly.

Suppose that we take a partition  $B_1 \cup B_2 \cup \dots \cup B_N$  of the set  $\{i = 1, \dots, I\}$ , and, at the  $k$ th step of the iteration, we use only a single  $B_n$ .

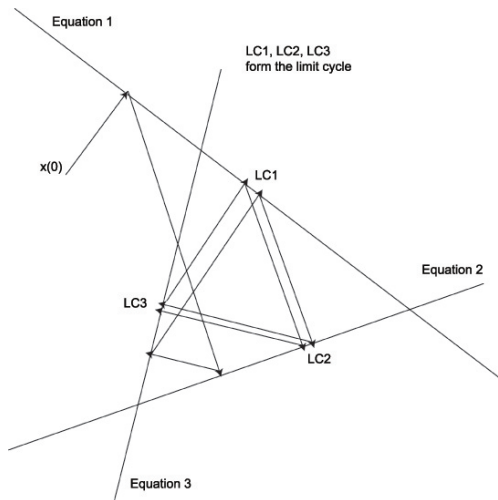
# The Ordered-Subset EM

At the  $k$ th step of the OSEM we compute

$$x_j^{k+1} = x_j^k s_{n,j}^{-1} \sum_{i \in B_n} P_{ij} \left( \frac{y_i}{(P_X^k)_i} \right), \quad (20)$$

for  $n = k(\bmod N) + 1$  and  $s_{n,j} = \sum_{i \in B_n} P_{ij}$ . Although its mathematical foundations are a bit shaky, it has proven to be a useful clinical tool.

# Limit Cycle



# Limit Cycles

Without strong under-relaxation, algorithms such as ART, MART and the OSEM that use only some of the data at each step of the iteration cannot converge to a single vector in the *inconsistent case*. For MART and OSEM this means there is no non-negative solution of  $y = Px$ , while for ART it simply means  $Ax = b$  has no solution. In such cases, these algorithms exhibit subsequential convergence to a limit cycle of (usually)  $N$  distinct vectors. One problem with OSEM is that it sometimes produces a limit cycle, even when there is a non-negative solution of  $y = Px$ . This makes the OSEM images noisier than they need to be, when the data is noisy.

# Rescaled Block-Iterative Reconstruction

The *rescaled block-iterative* EMML (RBI-EMML) is similar to the OSEM, but converges to a non-negative solution of  $y = Px$ , whenever such solutions exist, for every starting vector  $x^0 > 0$  and every choice of blocks. Let  $x^0$  be an arbitrary positive vector. For  $k = 0, 1, \dots$ , let  $n = k(\bmod N) + 1$ . Then let

$$x_j^{k+1} = (1 - m_n^{-1} s_j^{-1} s_{n,j}) x_j^k + m_n^{-1} s_j^{-1} x_j^k \sum_{i \in B_n} (P_{ij} \frac{y_i}{(Px^k)_i}), \quad (21)$$

with

$$m_n = \max\{s_{n,j} s_j^{-1} \mid j = 1, \dots, J\}.$$

# Entropy Maximization

When there are multiple non-negative solutions of  $y = Px$ , it makes sense to select the solution closest to a prior estimate of  $x$ , according to some measure of distance. The *cross-entropy* or Kullback-Leibler distance is frequently used. As we shall see, this distance is also closely related to the EMMML algorithm.

# The Kullback-Leibler Distance

The Kullback-Leibler distance between positive numbers  $\alpha$  and  $\beta$  is

$$KL(\alpha, \beta) = \alpha \log \frac{\alpha}{\beta} + \beta - \alpha.$$

We also define  $KL(\alpha, 0) = +\infty$  and  $KL(0, \beta) = \beta$ . Extending to non-negative vectors  $a = (a_1, \dots, a_J)^T$  and  $b = (b_1, \dots, b_J)^T$ , we have

$$KL(a, b) = \sum_{j=1}^J KL(a_j, b_j) = \sum_{j=1}^J \left( a_j \log \frac{a_j}{b_j} + b_j - a_j \right).$$

With  $a_+ = \sum_{j=1}^J a_j$ , and  $b_+ > 0$ , we have

$$KL(a, b) = KL(a_+, b_+) + KL(a, \frac{a_+}{b_+} b).$$

# The EMLL and Simultaneous MART

The EMLL algorithm has the iterative step

$$x_j^{k+1} = x_j^k s_j^{-1} \sum_{i=1}^I P_{ij} \left( \frac{y_i}{(P_X^k)_i} \right). \quad (23)$$

It is interesting to compare this iteration with that of the *simultaneous* MART (SMART):

$$x_j^{k+1} = x_j^k \exp \left[ s_j^{-1} \sum_{i=1}^I P_{ij} \log \left( \frac{y_i}{(P_X^k)_i} \right) \right]. \quad (24)$$

# Convergence and Open Questions

## Theorem

*The SMART sequence  $\{x^k\}$  converges to the non-negative minimizer of  $KL(Px, y)$  for which  $KL(x, x^0)$  is minimized, for any choice of  $x^0 > 0$ . The EMMML sequence  $\{x^k\}$  converges to a non-negative minimizer of  $KL(y, Px)$ , for any choice of  $x^0 > 0$ .*

It is an open question to which minimizer the EMMML sequence converges. In the consistent case, the limit is a non-negative solution of  $y = Px$ . If there are multiple non-negative solutions of  $y = Px$ , the limit will depend on  $x^0 > 0$ , but we do not know how it depends on  $x^0$ .

# SMART and Shannon Entropy

When  $y = Px$  has non-negative solutions, the SMART and MART algorithms produce sequences that converge to the unique non-negative solution that minimizes  $KL(x, x^0)$ , for any  $x^0 > 0$ . If  $x^0$  is the vector whose entries are all one, then minimizing  $KL(x, x^0)$  is equivalent to maximizing the *Shannon entropy*

$$SE(x) = \sum_{j=1}^J x_j (\log x_j) - x_j.$$

So the SMART and MART can be used to maximize entropy.

# The Split Feasibility Problem

Let  $A$  be a real  $I$  by  $J$  matrix, and  $C$  and  $Q$  non-empty closed, convex sets in  $R^J$  and  $R^I$ , respectively.

The *split feasibility problem* (SFP) is to find a vector  $x$  in  $C$ , such that  $Ax$  is in  $Q$ .

# The Inconsistent Case

When the SFP has no solution, it is sensible to seek a minimizer of the function

$$f(x) = \frac{1}{2} \|P_Q Ax - Ax\|_2^2, \quad (25)$$

over  $x$  in  $C$ ;  $P_Q$  denotes the orthogonal projection onto  $Q$ .

# The CQ Algorithm

For arbitrary  $x^0$  and  $k = 0, 1, \dots$ , and  $\gamma$  in the interval  $(0, 2/\rho(A^T A))$ , where  $\rho(A^T A)$  denotes the largest eigenvalue of the matrix  $A^T A$ , let

$$x^{k+1} = P_C(x^k - \gamma A^T(I - P_Q)Ax^k). \quad (26)$$

This is the CQ algorithm. The CQ algorithm converges to a solution of the SFP, whenever solutions exist. When there are no solutions of the SFP, the CQ algorithm converges to a minimizer, over  $x$  in  $C$ , of the function

$$f(x) = \frac{1}{2} \|P_Q Ax - Ax\|_2^2, \quad (27)$$

whenever such minimizers exist.

## Estimating $\rho(A^T A)$

The CQ algorithm employs the relaxation parameter  $\gamma$  in the interval  $(0, 2/\rho(A^T A))$ , where  $\rho(A^T A)$  is the largest eigenvalue of the matrix  $A^T A$ . Choosing the best relaxation parameter in any algorithm is a nontrivial procedure. Generally speaking, we want to select  $\gamma$  near to  $1/\rho(A^T A)$ . A simple estimate for  $\rho(A^T A)$  that is particularly useful when  $A$  is sparse is the following: if  $A$  is normalized so that each row has length one, then the spectral radius of  $A^T A$  does not exceed the maximum number of nonzero elements in any column of  $A$ . A similar upper bound on  $\rho(A^T A)$  was obtained for non-normalized,  $\epsilon$ -sparse  $A$ .

# The Multi-set SFP

Recently, Censor, Elfving, Kopf and Bortfeld have extended the CQ algorithm to the case in which the sets  $C$  and  $Q$  are the intersections of finitely many other convex sets. The new algorithm employs the orthogonal projections onto these other convex sets.

# Intensity-modulated Radiation Therapy

Censor, Bortfeld, Martin, and Trofimov use this new algorithm to determine intensity-modulation protocols for radiation therapy. The issue here is to determine the intensities of the radiation sources external to the patient, subject to constraints on how spatially varying the machinery permits these intensities to be, on the maximum dosage directed to healthy areas, and on the minimum dosage directly to the targets.

## Particular Cases of the SFP

It is easy to find important examples of the SFP: if  $C = R^J$  and  $Q = \{b\}$  then solving the SFP amounts to solving the linear system of equations  $Ax = b$ ; if  $C$  is a proper subset of  $R^J$ , such as the nonnegative cone, then we seek solutions of  $Ax = b$  that lie within  $C$ , if there are any. Generally, we cannot solve the SFP in closed form and iterative methods are needed.

# Particular Cases of the CQ Algorithm

A number of well known iterative algorithms, such as the Landweber and projected Landweber methods, are particular cases of the CQ algorithm.

# The Landweber Algorithm

With  $x^0$  arbitrary and  $k = 0, 1, \dots$ , the Landweber algorithm for finding a (possibly least-squares) solution of  $Ax = b$  has the iterative step

$$x^{k+1} = x^k + \gamma A^T(b - Ax^k). \quad (28)$$

# The Projected Landweber Algorithm

For a general nonempty closed convex  $C$ ,  $x^0$  arbitrary, and  $k = 0, 1, \dots$ , the projected Landweber algorithm for finding a (possibly constrained least-squares) solution of  $Ax = b$  in  $C$  has the iterative step

$$x^{k+1} = P_C(x^k + \gamma A^T(b - Ax^k)). \quad (29)$$

# The Simultaneous ART (SART)

Another example of the CQ algorithm is the *simultaneous algebraic reconstruction technique* (SART) of Anderson and Kak for solving  $Ax = b$ , for nonnegative matrix  $A$ . Let  $A$  be an  $M$  by  $N$  matrix with nonnegative entries. Let  $A_{m+} > 0$  be the sum of the entries in the  $m$ th row of  $A$  and  $A_{+n} > 0$  be the sum of the entries in the  $n$ th column of  $A$ . Consider the (possibly inconsistent) system  $Ax = b$ . For  $x^0$  arbitrary and  $k = 0, 1, \dots$ , let

$$x_n^{k+1} = x_n^k + \frac{1}{A_{+n}} \sum_{m=1}^M A_{mn} (b_m - (Ax^k)_m) / A_{m+}. \quad (30)$$

This is the SART algorithm. With a change of variables, the SART becomes a particular case of the Landweber iteration

## Changing Variables

We make the following changes of variables:

$$B_{mn} = A_{mn}/(A_{m+})^{1/2}(A_{+n})^{1/2}, \quad (31)$$

$$z_n = x_n(A_{+n})^{1/2}, \quad (32)$$

and

$$c_m = b_m/(A_{m+})^{1/2}. \quad (33)$$

Then the SART iterative step can be written as

$$z^{k+1} = z^k + B^T(c - Bz^k). \quad (34)$$

This is a particular case of the Landweber algorithm, with  $\gamma = 1$ . The convergence of SART follows, once we know that the largest eigenvalue of  $B^T B$  is less than two; in fact, it is one.

# Proximal Minimization

The CQ algorithm is a particular case of an iterative algorithm based on Moreau's notion of proximity operator.

# Proximity Operators

The Moreau envelope of a convex function  $f$  is the function

$$m_f(z) = \inf_x \left\{ f(x) + \frac{1}{2} \|x - z\|_2^2 \right\}, \quad (35)$$

which is also the infimal convolution of the functions  $f(x)$  and  $\frac{1}{2} \|x\|_2^2$ . It can be shown that the infimum is uniquely attained at the point denoted  $x = \text{prox}_f z$ . The function  $m_f(z)$  is differentiable and  $\nabla m_f(z) = z - \text{prox}_f z$ . The point  $x = \text{prox}_f z$  is characterized by the property  $z - x \in \partial f(x)$ . Consequently,  $x$  is a global minimizer of  $f$  if and only if  $x = \text{prox}_f x$ .

# The Conjugate Function

The conjugate function associated with  $f$  is the function  $f^*(x^*) = \sup_x (\langle x^*, x \rangle - f(x))$ . In similar fashion, we can define  $m_{f^*} z$  and  $\text{prox}_{f^*} z$ . Both  $m_f$  and  $m_{f^*}$  are convex and differentiable.

# Moreau's Theorem

## Theorem

Let  $f$  be a closed, proper, convex function with conjugate  $f^*$ .  
Then

$$m_f z + m_{f^*} z = \frac{1}{2} \|z\|^2;$$

$$\text{prox}_f z + \text{prox}_{f^*} z = z;$$

$$\text{prox}_{f^*} z \in \partial f(\text{prox}_f z);$$

$$\text{prox}_{f^*} z = \nabla m_f(z), \text{ and}$$

$$\text{prox}_f z = \nabla m_{f^*}(z).$$

(36)

## An Example

For example, consider the indicator function of the convex set  $C$ ,  $f(x) = \iota_C(x)$  that is zero if  $x$  is in the closed convex set  $C$  and  $+\infty$  otherwise. Then  $m_f z$  is the minimum of  $\frac{1}{2}\|x - z\|_2^2$  over all  $x$  in  $C$ , and  $\text{prox}_f z = P_C z$ , the orthogonal projection of  $z$  onto the set  $C$ . The operators  $\text{prox}_f : Z \rightarrow \text{prox}_f z$  are proximity operators. These operators generalize the projections onto convex sets, and, like those operators, are firmly non-expansive (Combettes and Wajs).

The support function of the convex set  $C$  is  $\sigma_C(x) = \sup_{u \in C} \langle x, u \rangle$ . It is easy to see that  $\sigma_C = \iota_C^*$ . For  $f^*(z) = \sigma_C(z)$ , we can find  $m_{f^*} z$  using Moreau's Theorem:

$$\text{prox}_{\sigma_C} z = z - \text{prox}_{\iota_C} z = z - P_C z. \quad (37)$$

# Using Moreau's Theorem

The minimizers of  $m_f$  and the minimizers of  $f$  are the same.  
From Moreau's Theorem we know that

$$\nabla m_f(z) = \text{prox}_{f^*} z = z - \text{prox}_f z, \quad (38)$$

so  $\nabla m_f z = 0$  is equivalent to  $z = \text{prox}_f z$ .

# Proximal Minimization

Because the minimizers of  $m_f$  are also minimizers of  $f$ , we can find global minimizers of  $f$  using gradient descent iterative methods on  $m_f$ .

Let  $x^0$  be arbitrary. Then let

$$x^{k+1} = x^k - \gamma_k \nabla m_f(x^k). \quad (39)$$

We know from Moreau's Theorem that

$$\nabla m_f z = \text{prox}_{f^*} z = z - \text{prox}_f z, \quad (40)$$

so that Equation (39) can be written as

$$\begin{aligned} x^{k+1} &= x^k - \gamma_k (x^k - \text{prox}_f x^k) \\ &= (1 - \gamma_k) x^k + \gamma_k \text{prox}_f x^k. \end{aligned}$$

It follows from the definition of  $\partial f(x^{k+1})$  that  $f(x^k) \geq f(x^{k+1})$ .

## Minimizing $F(x) = f_1(x) + f_2(x)$

Combettes and Wajs consider the problem of minimizing the function  $F(x) = f_1(x) + f_2(x)$ , where  $f_2(x)$  is differentiable and its gradient is  $\lambda$ -Lipschitz continuous. The function  $F$  is minimized at the point  $x$  if and only if

$$0 \in \partial F(x) = \partial f_1(x) + \nabla f_2(x), \quad (42)$$

so we have

$$-\gamma \nabla f_2(x) \in \gamma \partial f_1(x), \quad (43)$$

for any  $\gamma > 0$ . Therefore

$$x - \gamma \nabla f_2(x) - x \in \gamma \partial f_1(x). \quad (44)$$

From Equation (44) we conclude that

$$x = \text{prox}_{\gamma f_1}(x - \gamma \nabla f_2(x)). \quad (45)$$

This suggests an algorithm, called the *forward-backward splitting* for minimizing the function  $F(x)$ .

# Forward-Backward Splitting

Beginning with an arbitrary  $x^0$ , and having calculated  $x^k$ , we let

$$x^{k+1} = \text{prox}_{\gamma f_1}(x^k - \gamma \nabla f_2(x^k)), \quad (46)$$

with  $\gamma$  chosen to lie in the interval  $(0, 2/\lambda)$ . The operator  $I - \gamma \nabla f_2$  is then averaged. Since the operator  $\text{prox}_{\gamma f_1}$  is firmly non-expansive, the sequence  $\{x^k\}$  converges to a minimizer of the function  $F(x)$ , whenever minimizers exist. It is also possible to allow  $\gamma$  to vary with the  $k$ .

# The CQ Algorithm as Forward-Backward Splitting

Recall that the split-feasibility problem (SFP) is to find  $x$  in  $C$  with  $Ax$  in  $Q$ . The CQ algorithm minimizes the function

$$f(x) = \|P_Q Ax - Ax\|_2^2, \quad (47)$$

over  $x \in C$ , whenever such minimizers exist, and so solves the SFP whenever it has solutions. The CQ algorithm therefore minimizes the function

$$F(x) = \iota_C(x) + f(x), \quad (48)$$

where  $\iota_C$  is the indicator function of the set  $C$ . With  $f_1(x) = \iota_C(x)$  and  $f_2(x) = f(x)$ , the function  $F(x)$  has the form considered by Combettes and Wajs, and the CQ algorithm becomes a special case of their forward-backward splitting method.

The End

THE END